Glaciers and Ice Sheets Mapping Orbiter concept

Kenneth Jezek,[1] Ernesto Rodríguez,[2] Prasad Gogineni,[3] Anthony Freeman,[2]
John Curlander,[4] Xiaoqing Wu,[4] John Paden,[3] and Chris Allen[3]

Received 30 August 2005; revised 10 November 2005; accepted 25 November 2005; published 13 May 2006.

[1] We describe a concept for a spaceborne radar system designed to measure the surface and basal topography of terrestrial ice sheets and to determine the physical properties of the glacier bed. Our primary objective is to develop this new technology for obtaining spaceborne estimates of the thickness of the polar ice sheets with an ultimate goal of providing essential information to modelers estimating the mass balance of the polar ice sheets and estimating the response of ice sheets to changing climate. Our new technology concept employs VHF and P-band interferometric radars using a novel clutter rejection technique for measuring surface and bottom topographies of polar ice sheets from aircraft and spacecraft. Our approach will enable us to reduce signal contamination from surface clutter, measure the topography of the glacier bed at better than 1 km intervals with an accuracy of 20 m, and paint a picture of variations in bed characteristics. The technology will also have applications for planetary exploration including studies of the Martian ice caps and the icy moons of the outer solar system. Through the concept developed here we believe that we can image the base and map the three-dimensional basal topography beneath an ice sheet at up to 5 km depth.

Citation: Jezek, K., E. Rodríguez, P. Gogineni, A. Freeman, J. Curlander, X. Wu, J. Paden, and C. Allen (2006), Glaciers and Ice Sheets Mapping Orbiter concept, *J. Geophys. Res.*, *111*, E06S20, doi:10.1029/2005JE002572.

1. Introduction

[2] Glaciers and ice sheets modulate global sea level by storing water deposited as snow on the surface and discharging water back into the ocean through melting and via icebergs. Only recently have we recognized, primarily from satellite observations, that the size of this frozen reservoir can change quickly as demonstrated by the rapid thinning of Jacobshavn Glacier in Greenland [*Thomas et al.*, 2003], Pine Island and Thwaites Glaciers in Antarctica [*Rignot*, 2001] and the demise of the Larsen Ice Shelf followed by thinning of interior Antarctic Peninsula Glaciers [*Scambos et al.*, 2004]. Yet none of these events are captured by current glaciological models suggesting that there are critical gaps in observations and theory about the dynamics of large ice sheets.

[3] Major observational gaps are associated with detailed knowledge of ice sheet basal topography and basal conditions. While much work has been done to measure ice thickness from aircraft, gaps in coverage remain especially over part of Antarctica [*Lythe et al.*, 2001; *ISMASS Committee*, 2004]. Very little information is available anywhere about variations in properties of the subglacial bed where we believe critical changes in the controls on ice sheet flow takes place. Recent technical advances suggest that this situation will change. During 2004 experiments at Summit Camp, Greenland [*Paden et al.*, 2004], we showed that it is possible to construct local, two-dimensional maps of basal reflectivity using a surface-based SAR approach [*Gogineni et al.*, 2005]. These tests demonstrate the first-ever successful imaging of the ice-bed interface through 3-km-thick ice with a monostatic SAR operating at incidence angles between 9° and 20°. We observed adequate signal-to-noise ratio both at 150 and 350 MHz. We also collected multiple phase history data sets along 3 km lines at 80, 150 and 350 MHz with HH polarization. These data were collected with offsets ranging from 2 to 10 m to study the use of an interferometric SAR to obtain additional basal topography data with fine resolution. Figures 1 and 2 show sample image results obtained with the SAR at 150 and 350 MHz, respectively. These images show variations of reflectivity caused by ice-bed physical characteristics as a function of along-track and cross-track position.

[4] The success of our Greenland experiments motivated us to develop the conceptual design of a new spaceborne sensor to measure the regional-scale three-dimensional topography beneath the polar ice sheets and to probe, systematically and comprehensively, the base of the polar ice sheets. We call the concept the Global Ice Sheet Mapping Orbiter (GISMO). We ultimately seek to perform pole-to-pole measurements of glacier and ice sheet thickness, basal topography, and physical properties of the glacier bed that will help to answer three fundamental

[1] Byrd Polar Research Center, Ohio State University, Columbus, Ohio, USA.
[2] Jet Propulsion Laboratory, California Institute of Technology, Pasadena, California, USA.
[3] Department of Electrical Engineering and Computer Science, University of Kansas, Lawrence, Kansas, USA.
[4] Vexcel Corporation, Boulder, Colorado, USA.

0148-0227/06/2005JE002572

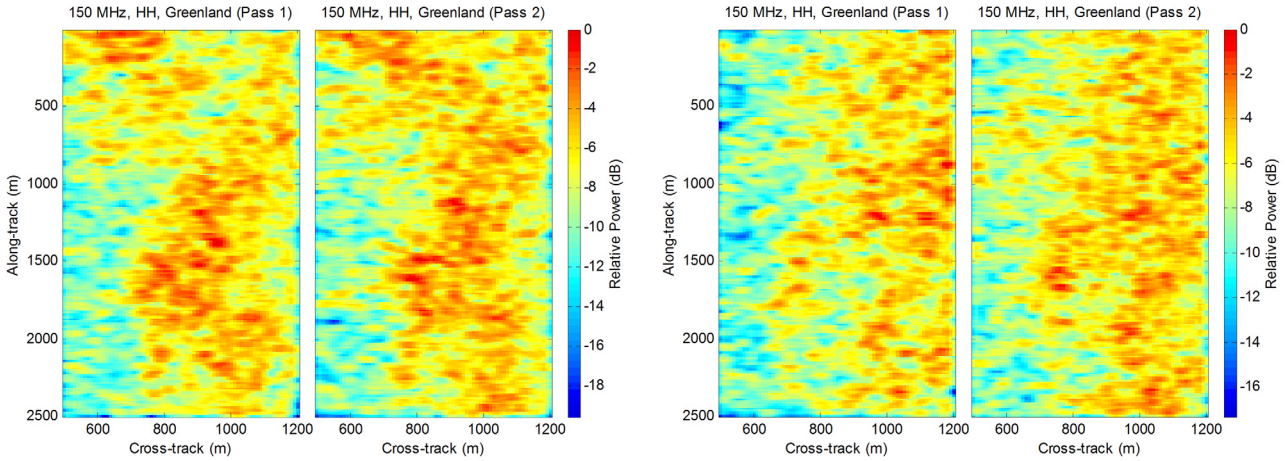

Figure 1. Monostatic synthetic aperture radar (SAR) images of the ice-bed interface at 150 MHz near Summit Camp, Greenland. Passes 1 and 2 refer to separate data collection passes over the same terrain.

questions: What is the impact of changing ice sheets on global sea level rise? Can we predict changes in ice sheet volume and hence changes in global sea level as global climate changes? Can scientific and technical lessons learned about Earth's ice cover be carried over to solving problems about icy bodies in the outer solar system?

[5] The conceptual design presented here offers two unique features compared to other spaceborne ice sounder designs: instead of providing one-dimensional profiles, a 50 km swath is imaged by each pass; it also uses radar interferometry in a novel way to remove the clutter contamination from the ice sheet surface. Previous spaceborne designs, such as the Europa sounder [*Blankenship et al.*, 1999], or the currently operating MARSIS sounder, provide only profiling measurements. These designs rely on synthetic aperture (or delay Doppler) processing to reduce the ice sheet clutter contribution from the ice sheet surface, but still suffer from clutter contamination in the cross-track direction. This clutter contamination is mitigated by increasing the antenna directivity (Europa sounder) or operating at very low frequencies (MARSIS).

2. Glaciological Measurement Parameters

[6] Our objective is to measure the three-dimensional properties of the base of the polar ice sheets, thereby giving us estimates of ice thickness and basal physical properties. Two concepts demonstrate the fundamental role of ice thickness and basal physical properties in understanding and predicting ice sheet behavior. The physical state of glaciers and ice sheets can be characterized in terms of their mass balance and dynamics. The mass balance is described by the depth-integrated mass-continuity equation given in terms of ice volume as

$$\frac{dh}{dt} = -\nabla \cdot H\mathbf{U} + a, \tag{1}$$

where h is the ice surface elevation, H is the ice thickness, $\mathbf{U}$ is the velocity and a is the accumulation rate. The left-hand side represents the change in ice elevation with time (assuming that the bed is fixed). It is best measured by altimeters that have now been operated over decadal intervals with great success. However, the altimeter measurements are susceptible to complications due to factors such as changes in the

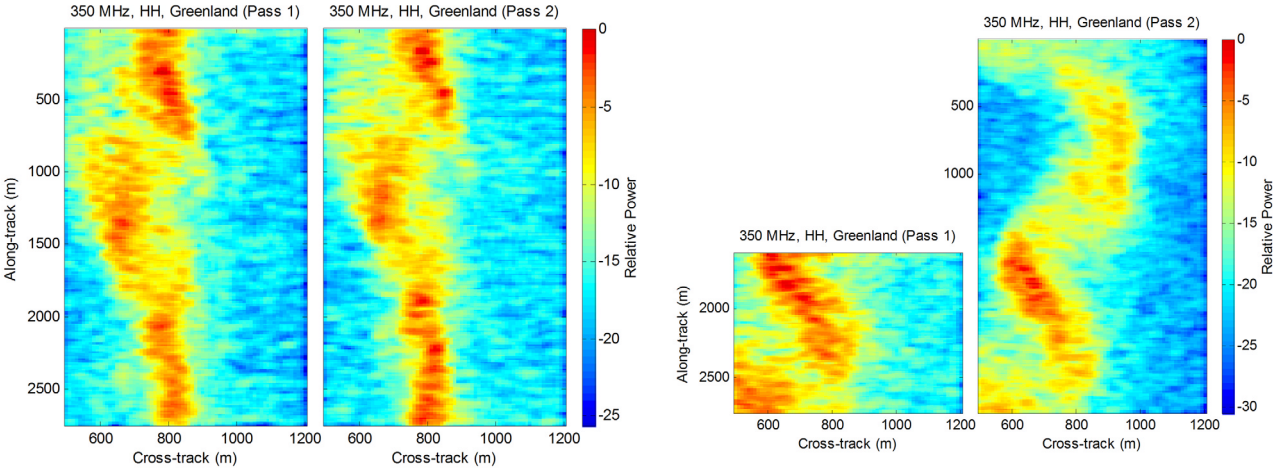

Figure 2. Monostatic SAR images of the ice-bed interface at 350 MHz near Summit Camp, Greenland. Passes 1 and 2 refer to separate data collection passes over the same terrain.

near surface density unrelated to changes in the mass balance. The right-hand side represents the state of balance between the outward flux of ice and the ice accumulated on the surface (or base). Because of measurement techniques, it can represent a slightly different estimate than that captured by altimeters. Point values of **U** as well as spatial gradients in **U** and H do not react instantaneously to changes in surface temperature or accumulation rate. So mass balance estimated using surface velocities, accumulation rate and available estimates of ice thickness yield a mass balance estimate that reflects an averaging over time.

[7] Insight into the forces controlling ice sheet shape and motion comes from dynamical equations usually written in terms of equalities between depth-averaged stresses and gradients in depth integrated stress. For example, it is easily shown that for a simple model consisting of a glacier driven under its own weight and restrained by forces at the sides and the bottom that

$$\tau_d = \tau_b + \frac{H}{w}\tau_s,$$

where the driving stress (τ_d) is proportional to the product of ice thickness and surface slope, τ_s is side drag, w is the width of the glacier, and τ_b is the basal drag [*van der Veen*, 1999]. Information on τ_s can be computed from InSAR surface velocities and ice rheological properties. The driving stress is computed from altimeter derived surface slopes and available knowledge on ice thickness. The basal drag term is usually deduced.

[8] By combining equations describing the balance of forces in a glacier with knowledge about ice rheology and with the continuity equation, it becomes possible to build models that predict how changes in external climate forcings or internal forcings (such as changes in the amount of water at the base of a glacier) will change the mass balance. Of the variables needed to solve these equations, ice thickness and a priori information about the properties of the glacier bed (τ_b) are most poorly determined. Improving ice thickness and glacier bed knowledge will yield two important results. First, the right and left hand sides of the continuity equation can be solved separately using, on one hand, the results from spaceborne altimeters, and on the other hand, the results from spaceborne InSAR-derived velocity data, spaceborne passive microwave observations of accumulation rate along with the improved knowledge of ice thickness. The two estimates will not necessarily equate for the reasons given above and indeed the difference might tell something about the differences between the short-term and average state of ice sheet mass balance. Second, improved ice thickness and basal characteristics data will refine our understanding of the forces acting on glaciers. This information will provide modelers with a considerably enhanced data set for estimating future changes in global glacier cover and its contribution to sea level rise [*Wu and Jezek*, 2004].

3. Glaciers and Ice Sheets Mapping Orbiter (GISMO) Description

3.1. Conceptual Measurement System Technology

[9] We envision a unique spaceborne interferometric sounder instrument for obtaining information that will contribute to the understanding of polar ice sheets and glaciers sufficiently to assess their contribution to global sea level rise. The sounder will operate at VHF (130 MHz) and P-band (430 MHz) in interferometric mode at incidence angles near nadir. It will consist of two antennas for interferometric imaging of ice sheets from a spacecraft in a polar orbit. We will employ a novel filtering scheme applied to the interferograms to remove surface clutter and to obtain swath coverage of basal topography and basal reflectivity. The instrument design is such that it can operate in nadir mode or swath mode at incidence angles near nadir and can collect interferometric data in single-pass mode with two antennas or repeat-pass mode. We specify the system in terms of the following observational goals: (1) determine total global ice sheet volume by mapping surface and basal topography; (2) determine basal boundary conditions from radar reflectivity; and (3) understand the phenomenology of radar sounding of ice for applications to planetary studies.

[10] Our instrument concept is designed to meet the following measurement requirements: (1) measure ice thickness and basal topography to an accuracy of 20 m or better; (2) measure ice thickness every 1000 m (in some cases 500 m); (3) measure ice thickness ranging from 100 m to 5 km; (4) measure radar reflectivity from basal interfaces (relative 2 dB); and (5) pole-to-pole observations.

3.2. Technical Approach

[11] Current systems designed to map the basal topography and physical properties of the polar ice sheets are limited in three fundamental ways [*Gogineni et al.*, 1998]. First, aircraft supported missions are largely incapable of providing continental-scale coverage in Antarctica because of the limited number of bases from which to operate. Second, the systems typically collect data along profiles so that three-dimensional information must be gleaned from interpolation. Third, systems presently in use suffer signal degradation by surface clutter particularly in more dynamic areas of the ice sheet where the ice surface is rough. The later is one of the main reasons why airborne sounding radars are flown at low altitudes. For low-altitude airborne sounders, surface clutter appears at large incidence angles and can be rejected by means of the antenna pattern. Surface clutter is a much more severe problem for orbital sounding of polar ice sheets. For spaceborne sounders, the surface clutter appears at small incidence angles and the antenna dimensions (on the order of 100 m at VHF) required to reject the clutter by narrowing the cross-track resolution, are beyond the capabilities of current technology. The poor cross-track resolution inherent in a realizable antenna dimension poses a major challenge for obtaining adequate surface clutter rejection for spaceborne sounding of polar ice sheets. In addition, conventional sounding yields only one dimensional along-track transects, and obtaining suitable spatial coverage in the cross-track direction requires long (and expensive) missions. Subsurface soundings of Mars and the ice moons of Jupiter also pose similar challenges.

3.2.1. Spaceborne Mission Instrument Description

[12] We offer a novel interferometric system concept capable of overcoming the surface clutter problems and enabling two-dimensional swath mapping of the polar regions in a short-duration mission. These attributes lead

Table 1. Spaceborne System

Parameters	Value
Number of channels (polarimetric)	4
Center frequency, MHz	430
Bandwidth, MHz	6
Pulse length, μsec	20
Peak transmit power, kW	5
Orbit repeat, weeks	2
Orbit type	polar
Platform height, km	600
One-look azimuth resolution, m	7
Pulse repetition frequency, kHz	10
Antenna diameter, m	12.5
Antenna type	mesh reflector
Boresight angle, deg	2.5
Interferometric baseline, m	45
Resolution after taking looks, km	1
Minimum number of looks	500

to significant gains in science capability over current approaches. Our conceptual system consists of a synthetic aperture radar interferometer (InSAR) operating at P-band using a 45 m interferometric baseline and at VHF. We restrict data collection to near nadir incidence angles leading to a 50 km swath that starts at a cross-track distance of 10 km from the nadir track. Table 1 presents detailed system parameters.

[13] Figure 3 presents the expected signal-to-noise and signal-to-clutter performance for 2-km-thick ice and Table 2 presents a detailed sample calculation for a pixel 25 km away from the nadir track. We selected two absorption values (9 and 18 dB/km) to model warmer and colder ice. In the near-nadir regime, one can model both the basal and ice surface backscatter cross section using the geometrical optics approximation [*Tsang et al.*, 1985]:

$$\sigma_0 = \frac{|R|^2 \exp[-\tan^2\theta/s^2]}{s^2 \cos^4\theta},$$

where R is the Fresnel reflection coefficient, θ is the incidence angle, and s is the surface RMS slope (at the wavelength scale). In our calculations, we assume that the Fresnel reflection coefficient squared at the basal layer is −11.4 dB at midswath (corresponding to a basal index of refraction of 3. and an ice index of refraction of 1.8), the basal layer has an RMS slope of 10°, and the ice surface has a slope of 1°, 3°, and 9°. Although the basal layer and ice surface P-band near-nadir cross sections or surface slopes are not well measured, indications from the analysis of sounder data show that the numbers used here are not optimistic. However, it may be possible that locally one may encounter rougher surfaces, leading to smaller signal-to-noise ratios.

[14] Given these assumptions, satisfactory signal-to-noise ratios are achieved for ice depths up to 4 km. Clutter contributions are the primary noise sources to the signal over the swath. The following section discusses how we plan to remove clutter and make decisions about final system parameters. Here, we briefly discuss the system design.

[15] An off-nadir swath requires an interferometric radar to estimate height. The height accuracy that can be achieved with an interferometer depends on the signal-to-noise (SNR) and signal-to-clutter (SCR) ratios, the number of radar looks, and the interferometric baseline [*Rodríguez and Martin*, 1992; *Rosen et al.*, 2000]. Modifying the equations in those references to include ray bending and the presence of a second surface that generates clutter contamination, we can derive the expected retrieved height accuracy as a function of SNR and SCR (E. Rodríguez and X. Wu, Interferometric ice sounding: A novel method for clutter rejection, submitted to *IEEE Transactions Geoscience and Remote Sensing*, 2005; hereinafter referred to as Rodríguez and Wu, submitted manuscript, 2005). Figure 4 shows the expected performance of the system given the parameters in Table 1. It also shows that, due to the large number of looks

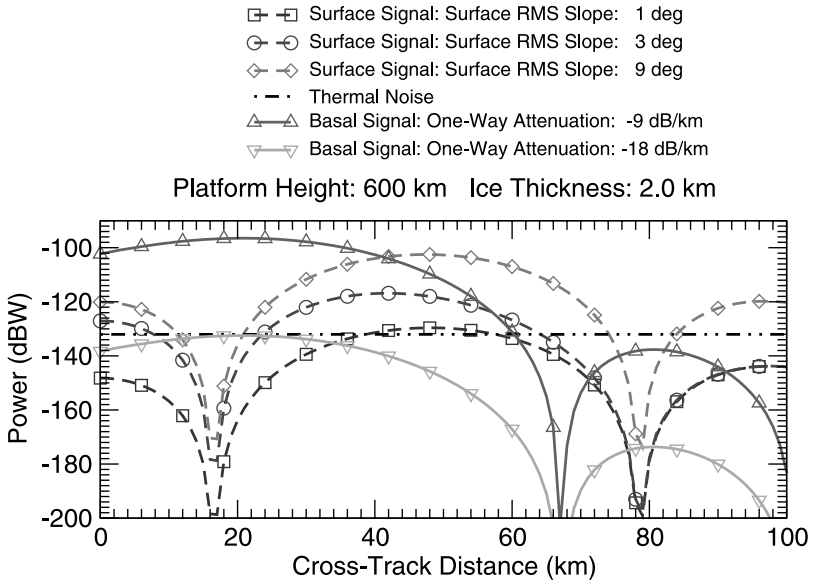

Figure 3. Expected signal-to-noise (SNR) and signal-to-clutter (SCR) ratios for an ice thickness of 2 km and for various surface clutter (which depends on the RMS slope of the ice sheet surface) scenarios. As can be seen from this figure, the instrument performance is limited by the clutter.

Table 2. Point SNR

Parameters	Units	Basal Return (9 dB/km Attenuation, 2 km Depth)	Ice Surface Return (3° Slope)
	Signal		
Peak power	dBW	+37.0	+37.0
$\chi^2/(4\pi)^3$	dBm^2	−36.1	−36.1
Transmit gain	dB	+33.0	+6.1
$1/r^4$	dBm^{-4}	−231.2	−231.2
σ_0	dB	+3.7	−6.5
Scattering area	dBm^2	+35.7	+31.3
Receive gain	dB	+33.0	+6.1
SAR compression gain	dB	+37.3	+37.3
Pulse compression gain	dB	+20.8	+20.8
System losses	dB	−3.0	−3.0
Medium attenuation	dB	−36.0	+0.0
Presumming gain	dB	+9.2	+9.2
Total signal power	**dBW**	**−96.7**	**−129.1**
	Noise		
Boltzmann's constant	dBWs/K	−228.6	−228.6
System temperature	dBK	+28.8	+28.8
Bandwidth	dBHz	+67.8	+67.8
Total noise power	**dBW**	**−132.0**	**−132.0**
SNR		**+35.3**	**+2.9**

and the 1 km spatial resolution, an SNR between −5dB and 0 dB is sufficient for achieving the desired height accuracy out to 60 km cross track distance. It also shows that the clutter reduction need not be perfect: achieving rejection ratios so that the final SCR is in the range between −10 dB and 0 dB is sufficient to meet the science requirements.

[16] We have selected the system to operate at 430 MHz for several reasons: (1) antenna size reduction relative to systems that operate at frequencies typically used to sound polar ice; (2) baseline reduction so that it is achievable in a single spacecraft; (3) at P-Band, ionospheric distortion effects are approximately 10 times smaller than at VHF frequencies; and (4) field experiments have shown that the attenuation due to ice propagation is relatively constant over the frequency range from 100 to 500 MHz [*Paden et al.*, 2005]. The main disadvantage of P-band is higher surface clutter. We propose to show that the clutter problem can be solved using a P-band radar.

[17] We have selected a fully polarimetric system to allow for corrections due to ionospheric distortions and Faraday rotation. *Freeman* [2004] and *Freeman and Saatchi* [2004] have shown that using polarimetric returns, it is possible to correct for Faraday rotation based on estimates extracted directly from the radar signals. This ensures that we will not lose signal power due to Faraday rotation and will allow us to better understand the scattering behavior of the base of the ice sheet. Analysis also indicates that it is possible, even at fairly high levels of ionospheric disturbance, to achieve an azimuth resolution commensurate with our 1 km spatial resolution requirement [*Liu et al.*, 2003].

3.2.2. Interferogram Filtering for Clutter Cancellation

[18] The idea behind interferometric filtering for clutter reduction is based on the fact that scattering from ice sheets consists of three components: (1) ice-air interface and near surface density variations; (2) ice-bed interface; and (3) intermediate layers, due mainly to changes in conductivity. The intermediate layers are weakly scattering even in the specular direction (reflection coefficients of −60 to −80dB) and can be neglected at off-nadir incidence. Thus off-nadir scattering can be treated as resulting from two interfaces. The top interface is relatively smooth in the interior, whereas the bottom interface can exhibit varying degrees of roughness. Because the speckle from the two interfaces is not correlated, the average radar interferogram, a complex product between the two interferometric channels, can be modeled as the sum of the interferogram from the basal and surface layers. In the near-nadir direction, the basal fringes (which are due to scattering near nadir) will vary much faster with range (or cross-track distance) than fringes from the clutter (which is generated at larger angles). Basal layer slopes, and, to a lesser degree, ice sheet slopes, will modulate the fringe rate, but in the near nadir direction the main contribution to the fringe rate will be the flat surface term, and surface slopes only play a secondary role. Figure 5 shows the result of Fourier transforming the sum interferogram for our system.

[19] We assumed that the SCR is 0 dB and ice thickness varies between 1 km and 4 km. The results clearly show that the surface and basal mean interferograms are well separated in spatial frequency. Thus we can separate the two signals with an appropriate filter. The results presented are for flat ice and basal layers, but it can be shown that at near-nadir incidence, fringe rate due to changes in surface slope are much smaller than changes due to the incidence angle. Since the interferogram is a complex signal, positive and negative frequencies can be separated. Because interferometric phase has opposite sign for objects to the left or right of the nadir track, the complex spatial frequencies will also have opposite signs. Thus we can differentiate signals from

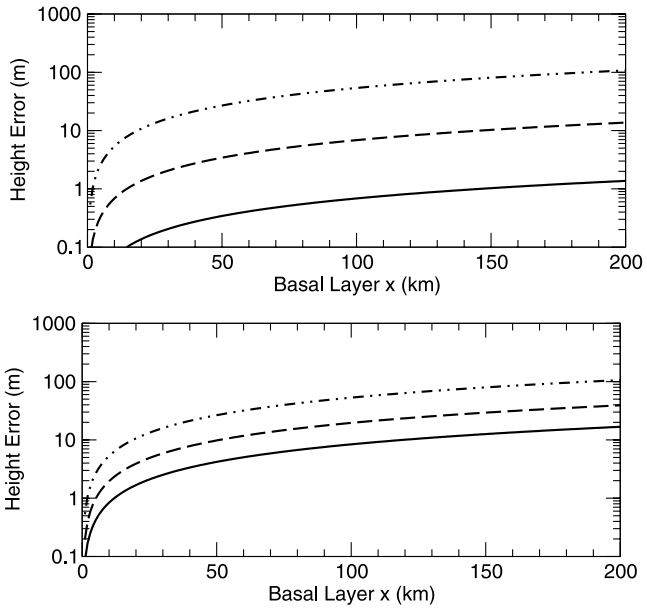

Figure 4. (top) Height error as a function of x, the cross-track distance of the basal return, and signal-to-clutter ratio (SCR) for values of 0 dB (solid line), −10 dB (long-dashed line), and −20 dB (dot-dashed line). (bottom) Height error cross the swath as a function of signal-to-noise ratio (SNR) values of 0 dB (solid line), −5 dB (long-dashed line), and −10 dB (dot-dashed line).

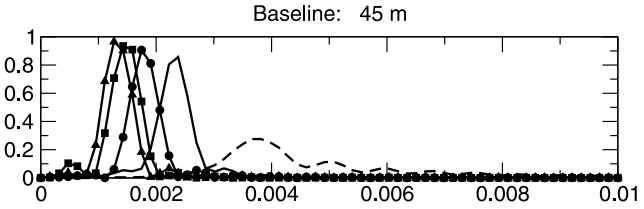

Figure 5. Spectrum of the interferogram for the basal return (dashed line) and for the surface return for ice depths of 1 km (solid line), 2 km (solid circles), 3 km (squares), and 4 km (triangles). The signal-to-clutter ratio has been assumed to be 0 dB. The spectral amplitude is in relative units. Only positive spatial frequencies are shown.

right and left of the nadir track by selecting the proper side of the Fourier spectrum.

[20] There are two complications with the spectral separation we show in Figure 5. First speckle noise for a single-look interferogram will generate signals at all spatial frequencies and mix signal and clutter. This effect can be mitigated using the fact that speckle noise can be reduced by multilooking interferograms. In our design, we take a substantial number (500 minimum) of looks so that the broadband speckle noise is substantially reduced. Although averaging results in a decrease of spatial resolution, it is still sufficient to meet the science requirements. Another potential problem arises due to the fact that the surface and basal reflectivities will have spatial variations, which will lead to spectral broadening. Surface scattering from the interior ice sheet is relatively homogeneous, so we expect that the spectral broadening of the surface return will be small. The basal return can have greater variability, but most of the broadening is expected at high frequencies so that we expect that the spectral separation will be maintained. Nevertheless, the exact magnitude of this corruption must be obtained by experimental measurements as is also the case for the actual magnitude of the SCR at P-band.

[21] At first glance, it might appear that we are extracting more information from the interferogram than is really there: after all, radar interferograms are traditionally used to derive heights only. However, we are using additional information not traditionally used in interferometry: namely, the spatial characteristics of the interferometric fringes. To make this useful, we have to assume that the scattering is effectively from only two surfaces. We also degrade the final spatial resolution relative to the instrument intrinsic spatial resolution. These sacrifices are not acceptable for most interferometric applications, but they are acceptable for our application over polar ice where the volume is only a source of weak scattering.

3.3. Simulation Results

[22] To investigate the interferometric technique under more complex situations, we did a phase history simulation based on the system parameters summarized in Table 1 and with a PRF of 2000 Hz. For the scene we selected a region in Greenland, where both surface and base digital elevation models (DEMs) are available from the National Snow and Ice Data Center. The ice mass is assumed to lie on rock with a permittivity of 9. The permittivity of 3.24 is used for the ice. A two-layer scene model is adopted, which means that the scattering characteristics within the ice mass and within the base beneath the ice mass is uniform and there are only two boundaries with permittivity discontinuities. One boundary is the top interface between the free air and the ice mass and the other is the bottom interface between the ice and the basal rocks. The attenuation within the ice mass is assumed to be 9 dB per one kilometer. The thickness of the ice mass varies from about 2000 to 2540 m. The scene averaged ice thickness is about 2270. The right-looking sensor was assumed to fly on an ascending orbit from south to north with an orbit inclination angle of 85°.

[23] Two independent steps were involved in the phase history simulation. The first step is to generate the reflectivity map of the scene according to the data acquisition geometry and the scattering properties of the scene. The received echo at the sensor for each pulse and each slant range bin is composed of surface and base contributions. The surface contribution comes from the backscattering of the transmitted signal from the radar on the air-ice interface. The basal contribution undergoes refraction through the ice mass, backscattering on the boundary between the ice mass and the base, and the refraction from the ice mass back to the free air. The second step is to create the phase history raw data from the reflectivity map for both the receiving antennas using the inverse chirp scaling algorithm.

[24] We then use VEXCEL's range Doppler SAR processor to process the raw data to single look complex (SLC) data and use VEXCEL's InSAR processor to create the interferogram, which is shown in Figure 6 after it is flattened. The interferogram is multilooked with 80 looks in azimuth direction and has both surface and basal contributions. Figure 7 shows the spectrum of the interferogram, where the x axis is the frequency of the fringes per slant range meter. The peak near the zero frequency represents the surface interferogram component and the other peaks on the right side are the result of the basal interferogram contribution. We extract the basal interferogram contribution from the mixed interferogram using a frequency domain band-pass filter. Figure 8 shows the filtered interferogram, which results mainly from the basal signal and so can be used to derive the basal topography and the ice mass thickness. Figure 9 shows the true ice thickness map. Figure 10 shows the ice thickness derived after applying the filtering scheme to the combined surface and basal interferogram. Figure 11 shows errors in the derived ice thickness map. The central part of the simulation area shows 0 to 20 m errors. The right-center areas show the largest errors, which are caused by the limitations in our band-pass filter and phase unwrapping schemes. The problems arise in this region from the fact that there is only minimal separation between the surface and basal topography spectra. This effect is expected from purely geometrical arguments, since as the incidence angle increases, the incidence angle for the surface and subsurface approach each other, and the fringe rates of the clutter and subsurface cannot be differentiated (Rodríguez and Wu, submitted manuscript, 2005). This limitation restricts the swaths that can be achieved from space to be smaller than about 50 km. In practice, this is a small restriction, since complete polar coverage at 60° latitude, can be achieved with fewer than 200 orbits leading to complete polar coverage approximately every 16 days. Additional artifacts are visible on the left sides of Figures 10

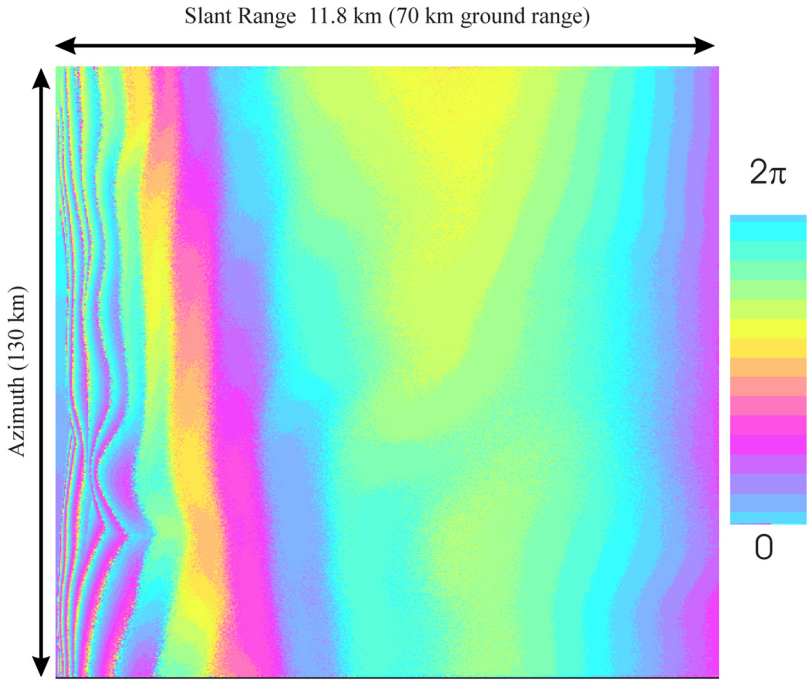

Figure 6. Interferogram from processing simulated phase history data for a region of Greenland with an average ice thickness of 2270 m. The interferogram was flattened with a smooth Earth surface and is multilooked with 80 azimuth looks.

and 11. These roughly vertically stripped patterns are caused by the particular frequency domain band-pass filter used in this study. A new time domain band-pass filter is under investigation (Rodríguez and Wu, submitted manuscript, 2005) to improve the quality of the filtered interferogram and to reduce such artifacts.

4. Conclusions

[25] We envision an instrument capable of generating swath maps of ice basal topography and reflectivity, a measurement not previously possible from space. Our concept is being developed to overcome limitations in conventional sounders that are profiling instruments. Their data consists of backscatter measurements as a function of return time, which can be interpreted as depth below the ice surface. Their spatial resolutions are typically limited by their bandwidth and viewing geometry (the pulse-limited footprint), which for spaceborne instruments is typically on the order of several kilometers.

[26] A further and greater limitation of spaceborne sounders is caused by the signal contamination due to surface clutter. Clutter suppression is very difficult to implement from space. For example, the ambiguous return for an ice depth of 1 km observed by a sounder from a height of 600 km would require that the antenna beam be much smaller than 3°. Assuming that one must be at least 2 to 3 beamwidths away from the main lobe to reach the appropriate level of clutter cancellation, this would require an antenna width of 30 m to 40 m at UHF frequencies and approximately 3 times larger at VHF. These antenna sizes, although conceptually realizable, are not yet mature and will likely lead to large mission costs due to launch vehicle and bus requirements. The technology we consider has significant advantages over other concepts for spaceborne sounders:

[27] 1. The conceptual system has a swath of 50 km. This will enable mapping of all latitudes above 60° with 200 passes (assuming ascending and descending data collection) which given a typical number of 14 passes per day would enable the collection of the entire polar regions above 60° in 16 days. This implies that with a mission lifetime of 3 months, one would be able to map Antarctica and Greenland about 6 times, to reduce random and systematic height errors. In comparison, assuming a profiling instrument of the desired resolution will require a total mission lifetime of about 4 years.

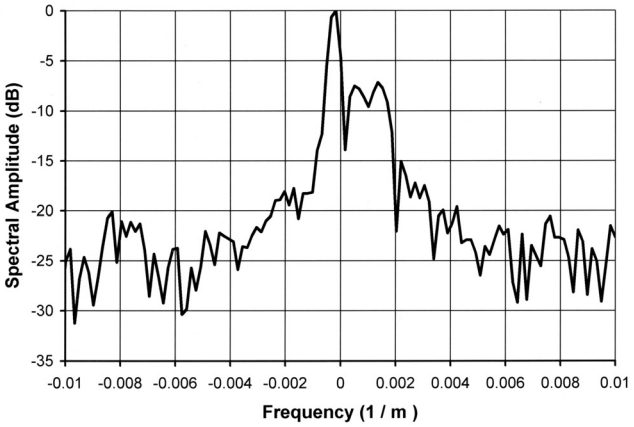

Figure 7. Spectrum of the interferogram in Figure 6. The peak near zero frequency represents the surface contribution, and the peaks at the right side are from the base. The *x* axis unit is the number of fringes per slant range meter.

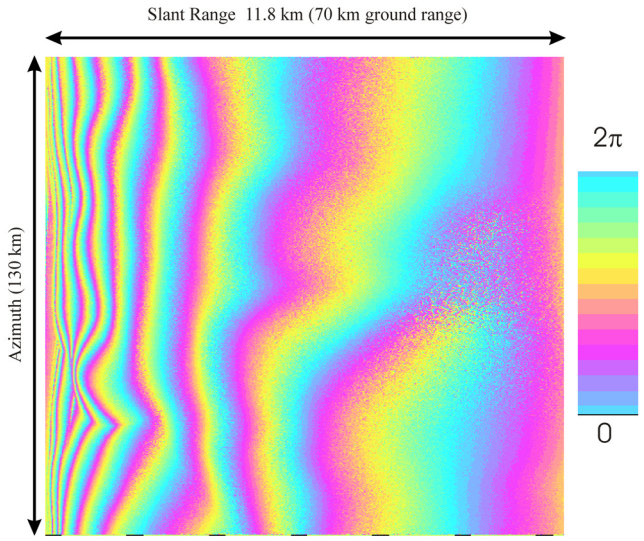

Figure 8. Band-pass-filtered interferogram derived from Figure 6. It mainly represents the basal interferogram contribution, which can be used to derive basal topography and the ice thickness.

[28] 2. The system concept we are advocating will require a 12.5 m diameter reflector antenna at P-band. These antennas have been successfully flown in space for telecommunication applications.

[29] 3. Sounder returns are maps of radar reflectivity as a function of depth that must be interpreted through waveform retracking to convert to basal depth. The interferometric measurement is a direct measurement of height. The estimated accuracy for single pass measurements is predicted to be better than 10 m, so that over a 3 month mission one could expect height accuracies on the order of 4 m or better (assuming uncorrelated errors).

[30] 4. The interferometric filtering technique presented above will allow for the separation of ice surface and basal signals. This is not possible with conventional sounding.

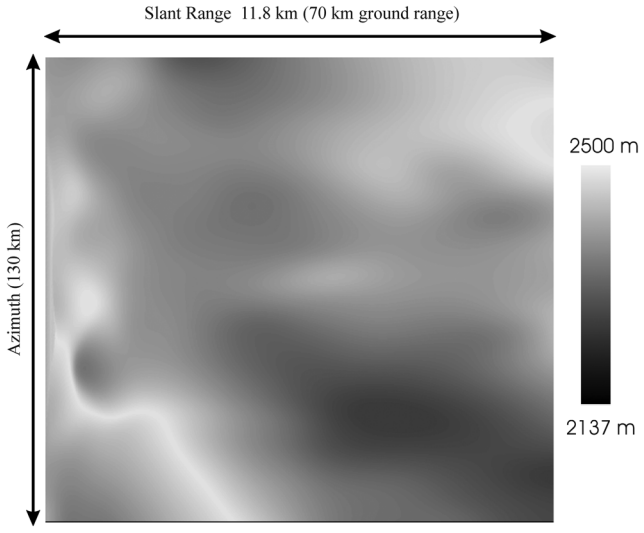

Figure 9. Ice thickness from the original digital elevation model.

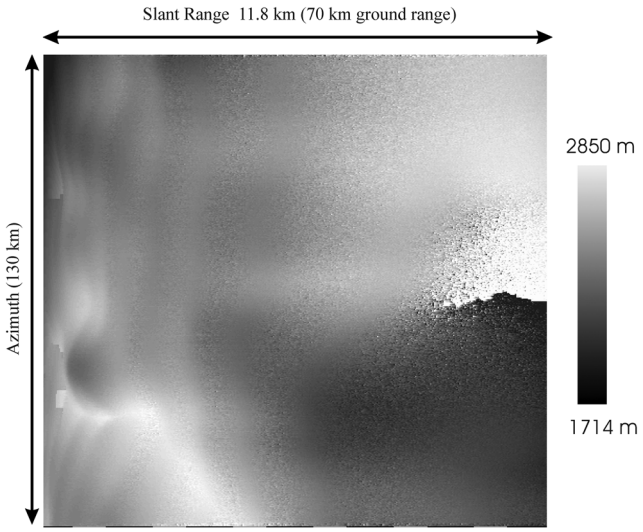

Figure 10. Ice thickness derived from the interferogram.

[31] 5. Our concept aims to produce three-dimensional information about the glacier bed. We recently succeeded in demonstrating that the base of the Greenland Ice Sheet could be successfully imaged with a 150 MHz radar operating on the ice sheet surface. While we are just beginning our interpretation of the images collected near the central ice divide of the ice sheet, the example demonstrates that backscatter variations from the ice sheet/bedrock interface are measurable.

[32] We also note that this technology has applications to the scientific exploration of extraterrestrial icy worlds. Surface clutter is a measurement obstacle common to studies of the Martian ice caps as well as to planned studies of the icy moons of the outer solar system. Our technical concept will find important applications for studying the dynamics of the Martian ice caps for and probing the volume of the ice shell suspected of enclosing a liquid ocean on Europa.

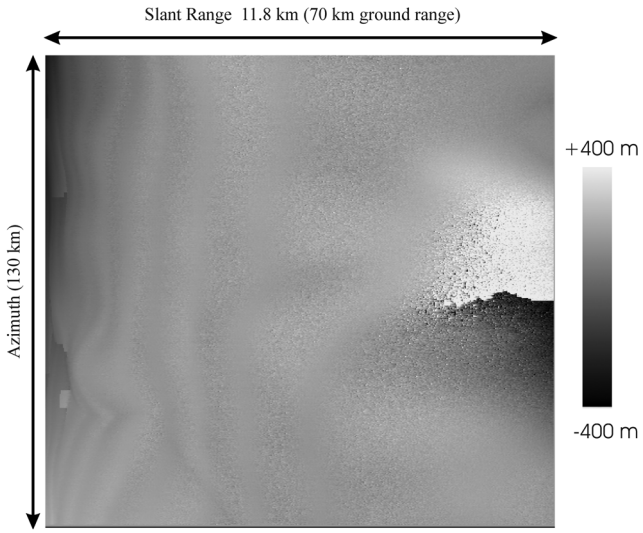

Figure 11. Ice thickness error map.

[33] **Acknowledgment.** This work is supported by a grant from the NASA Instrument Incubator Program.

References

Blankenship, D., et al. (1999), Feasibility study and design concept for an orbiting ice-penetrating radar sounder to characterize in three-dimensions the Europan ice mantle down to (and including) any ice/ocean interface, technical report, Jet Propul. Lab., Pasadena, Calif.

Freeman, A. (2004), Calibration of linearly polarized polarimetric SAR data subject to Faraday rotation, *IEEE Trans. Geosci. Remote Sens.*, *42*(8), 1617–1624.

Freeman, A., and S. S. Saatchi (2004), On the detection of Faraday rotation in linearly polarized L-band SAR backscatter signatures, *IEEE Trans. Geosci. Remote Sens.*, *42*(8), 1607–1616.

Gogineni, S., T. Chuah, C. Allen, K. Jezek, and R. K. Moore (1998), An improved coherent radar depth sounder, *J. Glaciol.*, *44*(148), 659–669.

Gogineni, S., K. Jezek, J. Paden, C. Allen, P. Kanagaratnam, and T. Akins (2005), Radar imaging and sounding of polar ice sheets, paper presented at XXVIIIth General Assembly of International Union of Radio Science, New Delhi.

ISMASS Committee (2004), Recommendations for the collection and synthesis of Antarctic Ice Sheet mass balance data, *Global Planet. Change*, *42*, 1–15.

Liu, J., Y. Kuga, A. Ishimaru, X. Pi, and A. Freeman (2003), Ionospheric effects on SAR imaging: A numerical study, *IEEE Trans. Geosci. Remote Sens.*, *41*(5), 939–947.

Lythe, M. B., D. G. Vaughan, and the BEDMAP Consortium (2001), BEDMAP: A new ice thickness and subglacial topographic model of Antarctica, *J. Geophys. Res.*, *106*(B6), 11,335–11,351.

Paden, J., S. Mozaffar, D. Dunson, C. Allen, S. Gogineni, and T. Akins (2004), Multiband multistatic synthetic aperture radar for measuring ice sheet basal conditions, in *Geoscience and Remote Sensing Symposium, 2004. IGARSS '04. Proceedings. 2004 IEEE International*, vol. 1, pp. 136–139, Inst. of Electr. and Electron. Eng., New York.

Paden, J. D., C. T. Allen, S. Gogineni, K. C. Jezek, D. Dahl-Jensen, and L. B. Larsen (2005), Wideband measurements of ice sheet attenuation and basal scattering, *IEEE Geosci. Remote Sens. Lett.*, *2*(2), 164–168.

Rignot, E. (2001), Evidence of rapid retreat and mass loss of Thwaites Glacier, West Antarctica, *J. Glaciol.*, *47*(157), 213–222.

Rodríguez, E., and J. M. Martin (1992), Theory and design of interferometric SARs, *Proc. IEEE*, *139*(2), 147–159.

Rosen, P. A., S. Hensley, I. Joughin, F. Li, S. Madsen, E. Rodríguez, and R. Goldstein (2000), Synthetic aperture radar interferometry—Invited paper, *Proc. IEEE*, *88*(3), 333–382.

Scambos, T. A., J. A. Bohlander, C. A. Shuman, and P. Skvarca (2004), Glacier acceleration and thinning after ice shelf collapse in the Larsen B embayment, Antarctica, *Geophys. Res. Lett.*, *31*, L18402, doi:10.1029/2004GL020670.

Thomas, R. H., W. Abdalati, E. Frederick, W. Krabill, S. Manizade, and K. Steffen (2003), Investigations of surface melting and dynamic thinning on Jacobshavn Isbrae, Greenland, *J. Glaciol.*, *49*(165), 231–239.

Tsang, L., J. Kong, and R. Shin (1985), *Theory of Microwave Remote Sensing*, Wiley-Interscience, Hoboken, N. J.

van der Veen, C. J. (1999), *Fundamentals of Glacier Dynamics*, 462 pp., A. A. Balkema, Brookfield, Vt.

Wu, X., and K. C. Jezek (2004), Antarctic ice-sheet balance velocities from merged point and vector data, *J. Glaciol.*, *50*(169), 219–230.

C. Allen, P. Gogineni, and J. Paden, Department of Electrical Engineering and Computer Science, University of Kansas, 2335 Irving Hill Road, Lawrence, KA 66045, USA.

J. Curlander and X. Wu, Vexcel Corporation, 4909 Nautilus Court, Boulder, CO 80301, USA.

A. Freeman and E. Rodríguez, Jet Propulsion Laboratory, California Institute of Technology, 4800 Oak Grove Drive, Pasadena, CA 91109, USA.

K. Jezek, Byrd Polar Research Center, Ohio State University, 108 Scott Hall, 1090 Carmack Road, Columbus, OH 43210, USA. (jezek.1@osu.edu)